Peculiarities of the formation of the structure of CMCs based on Al_2O_3 micropowder and SiC nanopowder in the process of electrosintering

A.G. Mamalis[1], E.S. Gevorkyan[2,3], M.M. Prokopiv[4], V.P. Nerubatskyi[2*], D.A. Hordiienko[2], D. Morozow[3], O.V. Kharchenko[4]

[1]Project Center for Nanotechnology and Advanced Engineering, Athens, Greece
[2]Ukrainian State University of Railway Transport, Kharkiv, Ukraine
[3]Kazimierz Pulaski University of Technology and Humanities in Radom, Poland
[4]V. Bakul Institute for Superhard Materials of the National Academy of Sciences of Ukraine, Kyiv, Ukraine

The influence of silicon carbide nanoadditives on the microstructure of the composite based on aluminum oxide microparticles during hot pressing due to electrosintering is investigated. The introduction of silicon carbide nanoparticles into the material leads to the formation of a specific structure of the material. A dispersion-strengthened nanocomposite of the "micro/nano" type is formed. On the other hand, all ceramic material containing granular silicon carbide powder is composite. In the process of sintering, a liquid phase is formed at a lower temperature, compared to the sintering of "micro-micro" particles. Such a complex structure of the composite leads to a significant improvement in the physical and mechanical properties of the material. In addition to the size of the SiC particles, the defects of the crystal lattice of the starting materials have a significant impact on the sintering and properties of the studied compositions. Nanodispersed silicon carbide powder has a more defective crystal lattice compared to the lattice of silicon carbide micropowder. The silicon carbide nanopowders used are more defective and, therefore, more active for sintering, since the process takes place under maximally non-equilibrium conditions. The microstructure obtained with different compositions of nanoadditives and sintering modes is studied. The peculiarities of the effect of various nanoadditives from Al_2O_3 and SiC on the microstructure and properties of the obtained materials were revealed. It was established that the use of this method makes it possible to improve such mechanical properties of the material as

microhardness (*HV* = 25.0 GPa) and crack resistance (KIC = 6.5 MPa·$m^{1/2}$).

Keywords: composite material, nanopowder, electrosintering, liquid phase, crack resistance, nanocomposite, ceramic matrix composite.

1. Introduction

Composite material based on Al_2O_3–SiC powders, due to its unique physical, mechanical and operational properties, has increasingly attracted many scientists specializing in materials science in recent years. Cheap and available on the market starting components made this material competitive compared to other known ceramic materials of this type. CMCs-composites Al_2O_3–SiC are promising as an instrumental and structural material. The creation of functionally gradient materials based on them will make it possible to further expand their prospective use [1–5]. The main trend in the development of modern composite materials, in particular instrumental materials, is to reduce material costs, respect ecology, and increase productivity.

CMCs based on aluminum oxide are interesting as tool materials with the greatest inertness to iron and are used mainly for processing carbon steels [6, 7]. Their main drawback is low strength and crack resistance [8]. The problem was solved by adding other compounds, in particular up to 20% TiC, TiN, TiCN and creating heterophase dispersion-strengthened ceramics by traditional hot pressing at 1600...1650 °C, and this is a high temperature – punches burn with the release of CO_2 [9, 10]. These materials provided clean and semi-clean turning, but did not provide a tendency to increase productivity due to an increase in cutting speed, because the temperature in the cutting zone increased due to insufficient thermal conductivity and strength of the cutting plates. To solve this problem, silicon carbide fibers can be added to aluminum oxide, which significantly increases the properties [11, 12].

Obtaining ceramic matrix composites based on aluminum oxide and silicon carbide by the method of electroconsolidation at temperatures at which chemical interaction occurs between the components with the formation of new phases both in the solid and in the liquid state makes it possible to obtain the maximum level of properties by various methods of hot pressing (electrosintering) [13, 14]. However, in this case, the technology of preservation of fibers during mixing during cold and hot pressing is somewhat complicated. An increase in the temperature of hot pressing leads to an increase in the cost of the material and deterioration of ecology [15, 16].

The use of silicon carbide nanopowder improves the mechanical properties of the composite, and also makes it possible to lower the temperature of hot pressing of the composite material [17]. At the same time, the traditional principles of materials science regarding the formation of the structure and properties of the material are preserved during hot pressing only for temperatures of 1400 °C and 1500 °C. At a temperature of 1600 °C, an increase in polytypes 6-H and IV (Si_7C_7) due to a decrease in the initial cubic polytype 3C was found in the material structure. A slight decrease in hardness and crack resistance was established. When the temperature of hot pressing is increased to 1700 °C, chemical interaction occurs between the components and the complete transformation of atomic 3C into 6H cells of silicon carbide and the formation of up to 4 wt.% SiO_2.

Despite the presence of the liquid SiO_2 phase (T_p = 1713 °C), the density of the material decreased by 5% compared to the density of samples obtained at temperatures of 1400 °C and 1500 °C. Disadvantages include the high temperature of the low-productivity method of

hot pressing for obtaining dense materials. One of the methods for solving this problem is the use of zirconium oxide in a stoichiometric ratio with Al_2O_3, which corresponds to the eutectic composition [18–20].

Today, the most successful material is based on Al_2O_3 micropowder and up to 15% micro- or nano-SiC [21–23]. At the same time, in the case of using micropowders, regardless of the parameters of the hot pressing process, the structure and properties of the material are formed on the basis of traditional materials science: the phase composition and their ratio correspond to the parameters of the original powder mixture. In the ceramic matrix composite CMCs, obtained on the basis of micropowders and nanopowders of Al_2O_3–SiC by the method of electroconsolidation, interesting transformations occur with the formation of a liquid phase and the disclosure of the features of the formation of the structure of this composite. This makes it possible to improve physical and mechanical properties, especially for the creation of promising functional gradient materials [24, 25].

2. Experimental conditions

The research used micropowders (1...2 μm) of α-Al_2O_3 produced by LLC "Khimlaboreaktiv" (Kyiv, Ukraine), as well as SiC nanopowder of the brand #4629HW manufactured by Nanostructured & Amorphous Materials (USA) CAS #409–21–2 (Fig. 1).

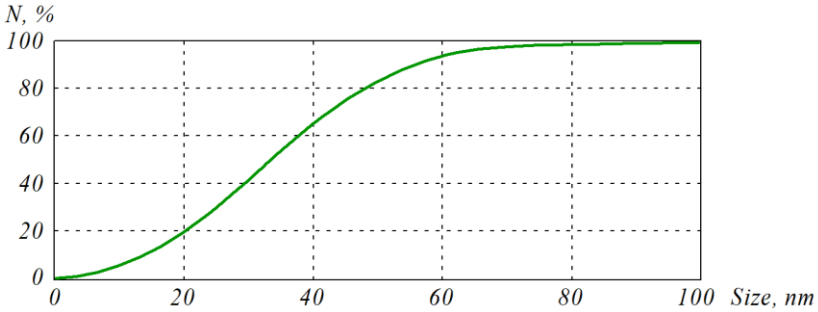

Figure 1. Particle size distribution of SiC100 powder

Basic information on the chemical composition of SiC nanopowder is given in Table 1.

X-ray phase analysis of these powders showed a clearly defined 3C-modification (cubic) phase and the presence of a small amount of 6H-modification (hexagonal) phase (Fig. 2, Fig. 3).

The results of analyzes of nano-SiC type powder show that the average size of SiC crystals is about 100 nm. The predominant phase of SiC is cubic 3C. Analysis of X-ray patterns and Raman scattering spectra indicates the presence of small amounts of the phase of the hexagonal polytype 6H-SiC and carbon.

Based on nano-SiC powder and nano (submicron) Al_2O_3 powder, charges were prepared for further compaction due to electroconsolidation.

Table 1. Chemical composition of SiC nanopowder

Parameter	Value
Color	gray-green
Crystalline form	cubic (3C)
Particle size, nm	80…100
Specific surface area, m^2/g	20…30
SiC content, %	99
Si, %	69.1

FSi, %	0.051
FC, %	0.35
Al, %	0.003
Mg, %	0.002
Fe, %	0.012
C, %	28.94
O, %	0.53
Ca, %	0.021

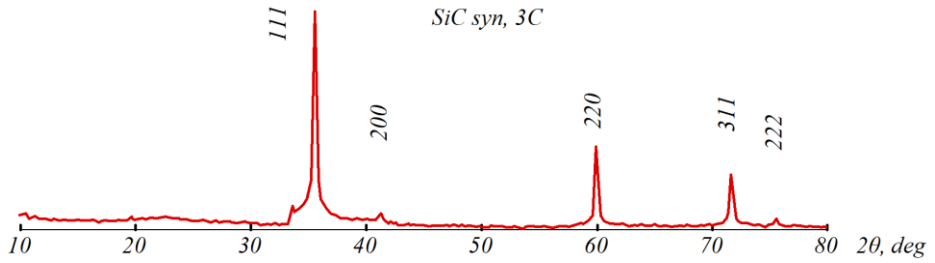

Figure 2. Diffractogram of SiC nanopowder

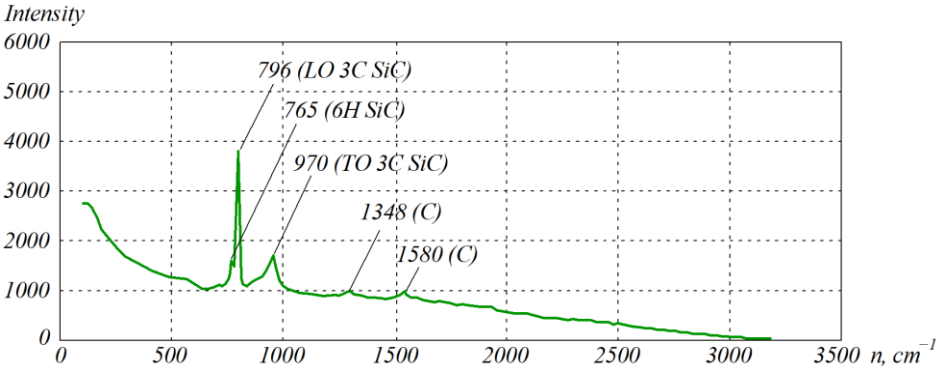

Figure 3. Raman spectrum of SiC nanopowder

According to the results of X-ray phase analysis, the charge consists of a mixture of Al_2O_3 with parameters a = 4.760 Å; c = 12.993 Å and SiC-3C with a lattice parameter a = 4.359 Å (Table 2).

The size of the coherent scattering region practically coincides and is 82.7 nm and 87.7 nm, respectively. Both Al_2O_3 and SiC are in a nanostructured state. The size of the coherent scattering region is 201.5 nm and 68.6 nm, respectively.

Table 2. Parameters of Al_2O_3–SiC powder mixtures

№ mixture	Phase	wt.%	Lattice parameters, Å	D, nm	ε
1	Al_2O_3	85.4	a = 4.760; c = 12.991	201.5	$3.4 \cdot 10^{-4}$
2	SiC-6H	14.6	a = 3.083; c = 15.110	68.6	$1.85 \cdot 10^{-3}$

On the diffractograms in Fig. 4, there are additional lines from petrolatum, which is used to bind powders, but the width of the lines is not affected.

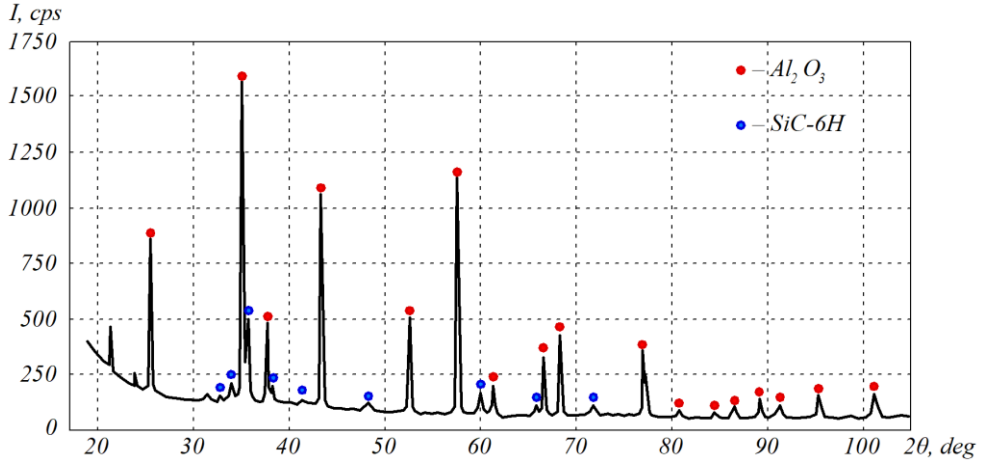

Figure 4. Diffractograms of powders with composition Al_2O_3–15 wt.% SiC

Mixing of the starting powders was carried out in a planetary mill "SAND" with a rotation frequency of 150 rpm in a medium of methyl alcohol for 2 hours. The duration of mixing was determined by the degree of obtaining a homogeneous distribution of powders in the mixture.

Samples for research were obtained in a hot pressing installation, which uses hot pressing by the electroconsolidation method [26, 27] at temperatures of 1400 °C, 1500 °C, 1600 °C, 1700 °C, as well as at T = 1760 °C.

Crack resistance was determined on the polished samples according to the Palqvist method [28, 29] under a load of P = 550 N on the Vickers pyramid. The hardness was determined by Rockwell on the TK-2 device and by Vickers under a load on the diamond pyramid P = 300 N. Microhardness was measured on the PMT3 device under a load of 2 N with simultaneous fixation of the microstructure and an impression from the Vickers pyramid. The chemical integral composition was determined using scanning electron microscope. X-ray microspectral studies of the local and integral composition of the structure of the sample obtained at 1760 °C were carried out using a scanning electron microscope "Carl Zeiss" (Germany).

3. Results and discussion

In Fig. 5 shows the surface structures of the samples in the optical image, which were obtained at temperatures of 1400 °C and 1500 °C. It should be noted that in the optical image of the structure of this material, the dark phase is aluminum oxide, and the light phase is silicon carbide.

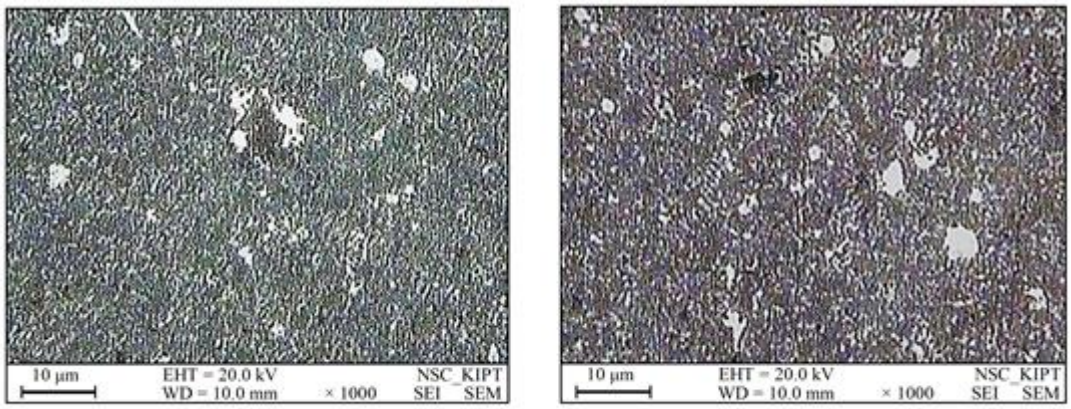

Figure 5. Image of the structure of the surface of the sample obtained at temperatures of 1400 °C, 1500 °C with exposure time of 3 min: (A) view of the structure of the extreme part of the surface of the cut sample, which is made at an angle of 2...3 degrees; (B) the middle of the sample with impressions from the Vickers pyramid

As can be seen from Fig. 5, the unprocessed surface of the sample has a characteristic uneven "bumpy" appearance, as after hot pressing, which makes it difficult to determine its structure. After diamond treatment removes the irregularities of this surface at an angle of 2...3° to a depth of 10^{-5} μm, it can be seen that the main structure (Figure 5, b) includes a dark-colored matrix phase with a small content of stochastically distributed dispersed inclusions 1...5 μm in size light phase. Individual grains of the light phase up to 20 μm in size were also found in the structure. As research has shown, the thickness of this surface layer is 30...50 μm. The hardness of *HV* is 18.7 GPa. The main structure also has a matrix phase, but lighter than the previous color, in which there are also dispersed inclusions of a light phase similar in size and distribution, but with a much smaller content.

At sintering temperatures exceeding 1800 °C, areas with a secondary eutectic microstructure formed from the liquid phase are found in the microstructure of the pressings (Fig. 6), which indicates locally inhomogeneous heating of the pressing material under the conditions of spark-plasma sintering. Analyzing visually the photographs of the structures of the samples obtained in the temperature range of 1400...1700 °C, we can say that they are of the same type in structure. The dark phase is the matrix, and the light phase is the dispersed particles of silicon carbide. Moreover, the size is in the range of 1...20 μm. That is, in the process of hot pressing, nanopowder of silicon carbide is formed in an aggregated state of light inclusions. There is a slight difference in the structure of the sample obtained at a temperature of 1760 °C.

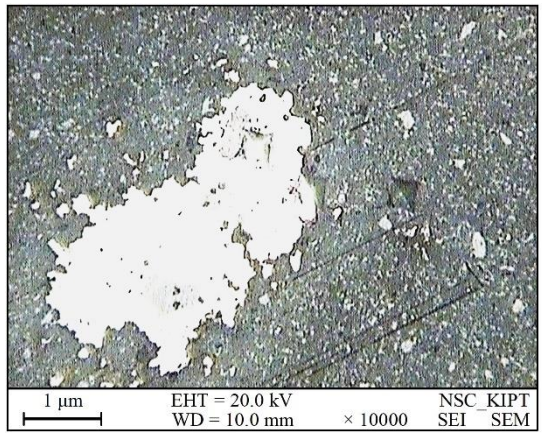

Figure 6. The microstructure obtained from a mixture of Al2O3 (micro)–15 wt.% SiC (nano) at a temperature of 1800 °C, a pressure of 35 MPa and a holding time of 3 min

In the temperature range of 1400...1700 °C, the structure in the center of the sample does not change and is a matrix of the dark-colored phase.

On the surface of the sample in Fig. 7, spots with a complex structural structure, as well as a light phase with dispersed inclusions of a dark and light gray phase, were detected.

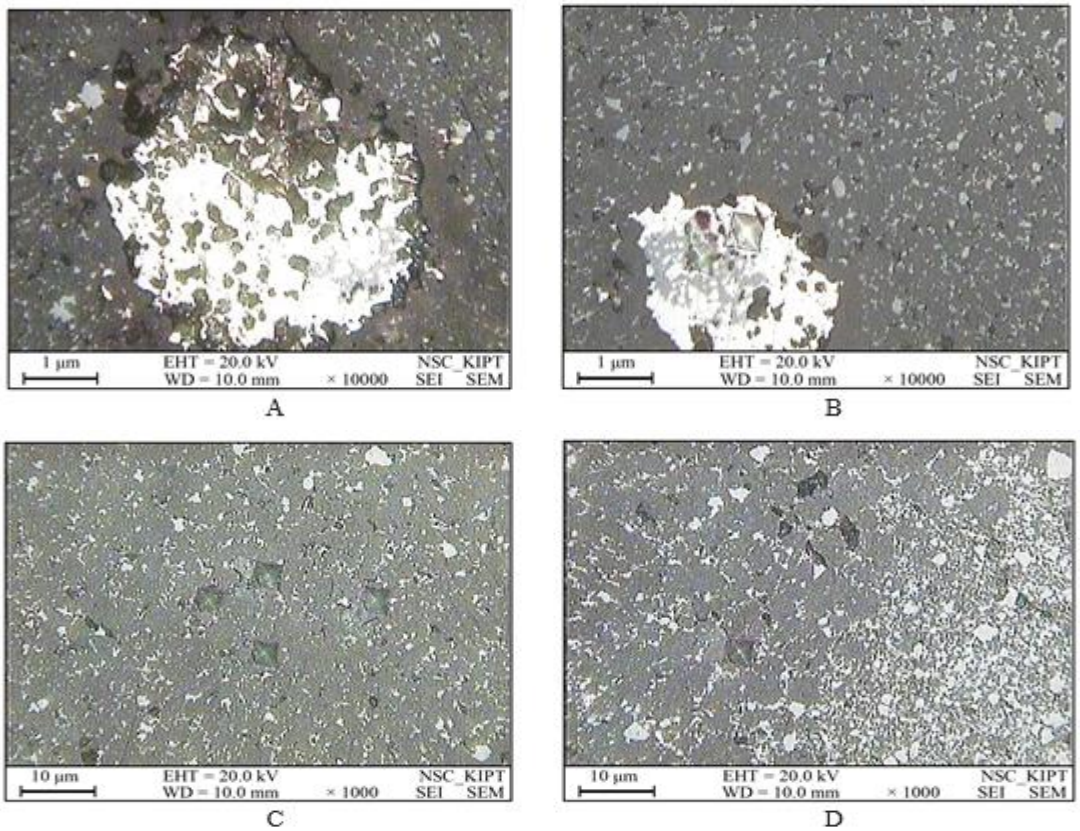

Figure 7. Structures of different parts of the surface of the sample obtained at a temperature of 1760 °C from a mixture of Al2O3 (micro)–15 wt.% SiC (nano): (A) and (B) aggregates of

SiC nanopowders; (C) and (D) hardness meter prints in different parts of the sample

In Fig. 8 shows that as a result of the formation of a liquid phase in the composite, silicon carbide particles are arranged in the form of mesh colonies.

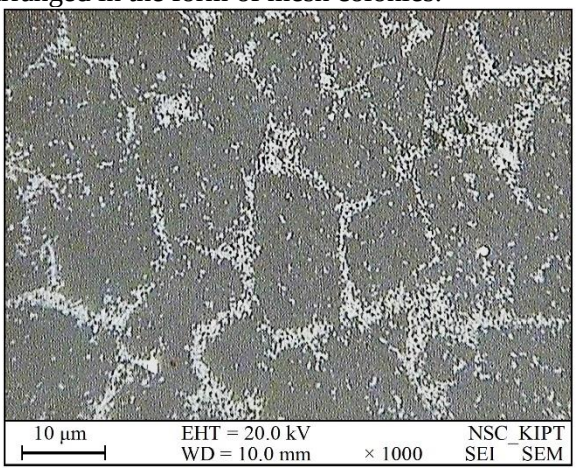

Figure 8. The surface structure of the sample obtained at a temperature of 1760 °C from a mixture of Al_2O_3 (micro)–15 wt.% SiC (nano)

In Table 3 shows the results of the integral chemical analysis of the elements in the structure of the samples depending on the sintering temperature.

The structure of the Al_2O_3 (micro)–15 wt.% SiC sample is shown in Fig. 9, and the micro X-ray spectral analysis of the sample is shown in Table 4. From the Table 4 shows that free carbon appears in the structures obtained at a temperature of 1700 °C.

Table 3. Integral chemical analysis of elements in the structure of samples

Sintering temperature, °C	C, %	O, %	Al, %	Si, %	Fe, %	W, %
1400	7.20	44.62	37.81	9.92	0.22	0.12
1500	6.92	44.81	37.69	9.85	0.66	0.06
1600	6.57	46.51	39.21	8.22	0.38	0.00
1760	3.31	47.85	40.92	6.23	0.06	1.63

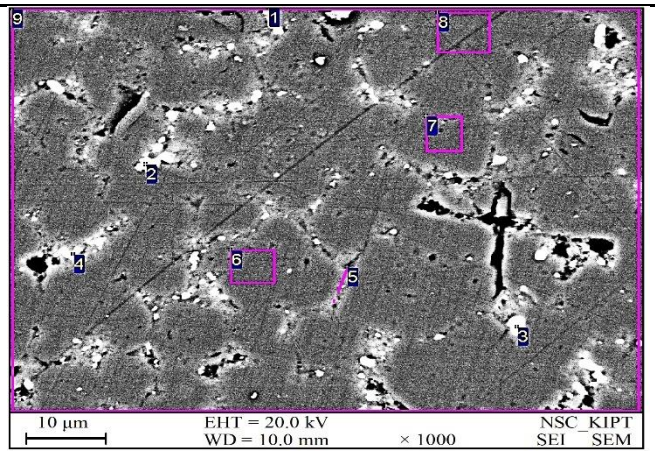

Figure 9. Structures of different parts of the surface of the sample obtained at a temperature of 1700 °C from a mixture of Al_2O_3 (micro)–15 wt.% SiC (nano)

Table 4. Results of chemical analysis of elements in the structure

Spectrum	C, %	O, %	Al, %	Si, %	Fe, %	Co, %	W, %
1	61.57	13.23	7.26	17.57	–	–	0.37
2	51.99	19.51	11.00	16.08	0.44	0.31	0.66
3	51.01	18.98	11.85	16.40	0.18	0.75	0.86
4	59.88	8.60	12.80	18.05	–	0.15	1.51
5	27.68	37.32	18.60	16.39	–	–	–
6	10.13	58.02	30.58	1.28	–	–	–
7	8.28	59.03	30.06	2.62	–	–	–
8	8.77	59.67	30.96	0.59	–	–	–
9	13.39	53.87	26.99	5.74	–	–	–

The structure obtained from a mixture of Al2O3 (micro)–15 wt.% SiC (nano) is shown in Fig. 10.

In the Table 5 shows the X-ray microspectral analysis of the sample area in squares 9 and 10.

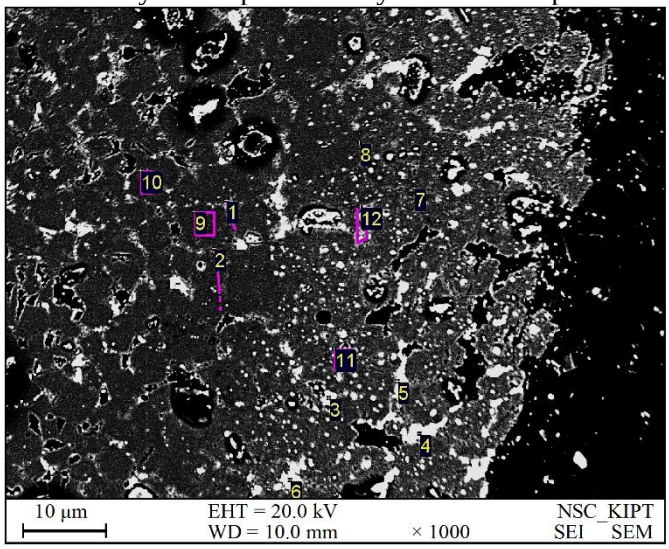

Figure 10. The structure obtained from a mixture of Al_2O_3 (micro)–15 wt.% SiC (nano)

Table 5. X-ray microspectral analysis of the sample area in squares 9 and 10

Spectrum	C, %	O, %	Al, %	Si, %	Ti, %	Co, %	W, %
1	27.78	38.08	19.33	14.80	–	–	–
2	13.53	52.62	29.93	3.93	–	–	–
3	58.04	–	3.49	37.77	–	–	0.71
4	59.14	2.40	3.57	34.16	0.73	–	–
5	41.73	26.47	9.57	21.81	0.13	–	0.29
6	62.57	6.55	7.41	22.05	0.22	–	1.20
7	29.34	44.29	20.36	6.02	–	–	–
8	19.93	47.67	24.38	8.02	–	–	–
9	8.88	59.31	30.09	1.73	–	–	–
10	9.37	58.49	30.61	1.53	–	–	–
11	24.40	43.06	22.83	9.72	–	–	–
12	39.16	27.44	14.24	18.97	–	0.18	0.01

In the case of using SiC nanopowder, the temperature of hot pressing of the material with maximum properties is decreases by 350...400 °C, while the traditional principles of materials science of the formation of the structure and properties of the material are

preserved during hot pressing only for temperatures of 1400 °C and 1500 °C.
At a temperature of 1600 °C, an increase in polytypes 6H and IV (Si_7C_7) due to a decrease in the initial cubic polytype 3C was found in the material structure (Fig. 11).
A slight decrease in hardness and crack resistance was established. Increasing the temperature of hot pressing to 1700 °C between the components leads to chemical interaction and complete transformation of the atomic 3C to 6H cell of silicon carbide and the formation of up to 3.26 wt.% SiO_2. Although it is generally known that the transition temperature is above 2000 °C. The reduction of aluminum oxide and silicon carbide directly indicates that silicon oxide was formed as a result of the interaction between them: Al_2O_3 – 82.85 wt.%; SiC-6H – 13.28 wt.%; SiO_2-stishovite – 3.26 wt.%; SiO_2-Quartz – 0.61 wt.%.

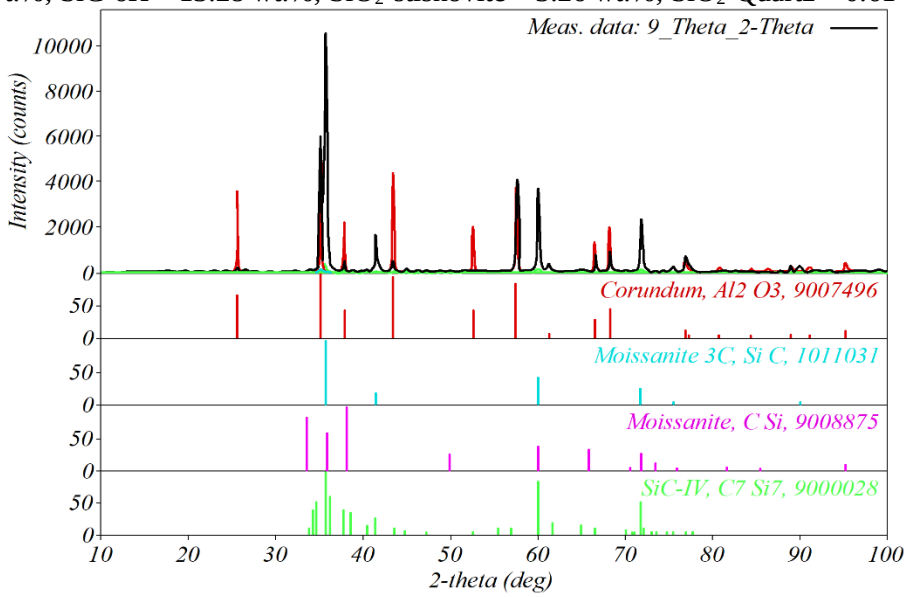

Figure 11. X-ray phase analysis of Al_2O_3–15 wt.% SiC composites obtained by hot pressing due to electrosintering at temperature T = 1600 °C, pressure P = 35 MPa, sintering time 2 min

Today, well-known materials are obtained from both macro- and micropowders of the original components by hot pressing at a temperature of T = 1800 °C, friction pairs have been created [30], as well as cutting plates for high-performance mechanical processing of alloys on based on iron. In the case of using micropowders during hot pressing at temperatures up to 1800 °C, a classic matrix-type structure is formed from Al_2O_3 with a SiC dispersed phase and the corresponding formation of a complex of properties (Table 6).

Table 6. Results of measurements of hardness and crack resistance of the Al_2O_3 sample

Sample temperature	Crack resistance K_{IC}, MPa·m$^{1\backslash 2}$	Hardness *HV* (15)
1500 °C	5.3	13.5 (edge)
1500 °C	5.1	14.0 (between them)
1500 °C	6,1	15.6 (center)
1400 °C	4.1	17.9 (edge)
1400 °C	5,3	18.8 (center)
1700 °C	4.1	16.0 (center)
1700 °C	4.5	14.6 (edge)

The research was carried out with loads on the Vickers pyramid – 15 kg. Some observations during the preparation of grinding samples on the ShP-3A planetary grinding and polishing machine.

At 1760 °C, a more uniform distribution of the light gray phase is observed, as well as a deformation from a round to an elongated shape. A sample made from a mixture of Al_2O_3 micro-15 wt.% (Fig. 12).

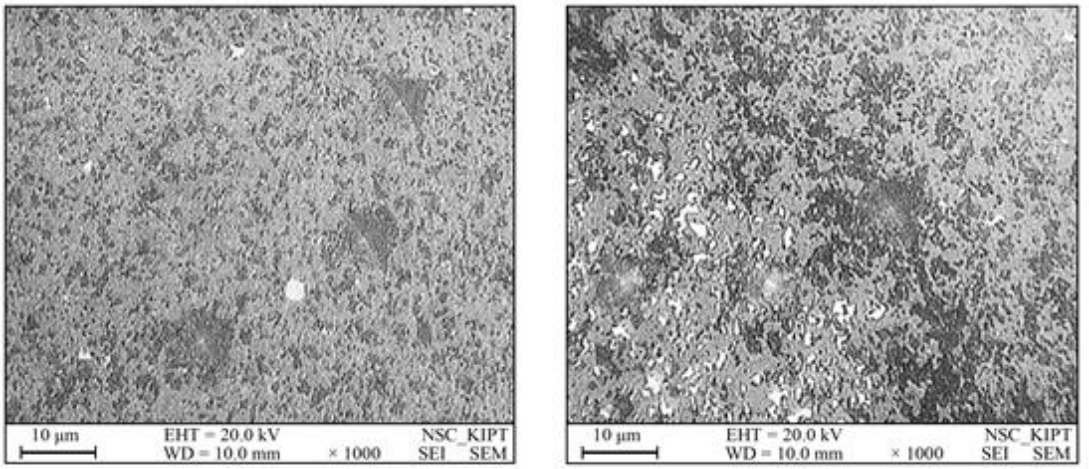

Figure 12. The structure obtained from a mixture of Al_2O_3 (micro)–15 wt.% SiC (nano) at a temperature of 1760 °C

As can be seen, compared to the initial composition, the mass fraction has changed, which is caused by chemical reactions. Thus, the SiO_2 phase is formed in the composition of the sample after consolidation (Fig. 13).

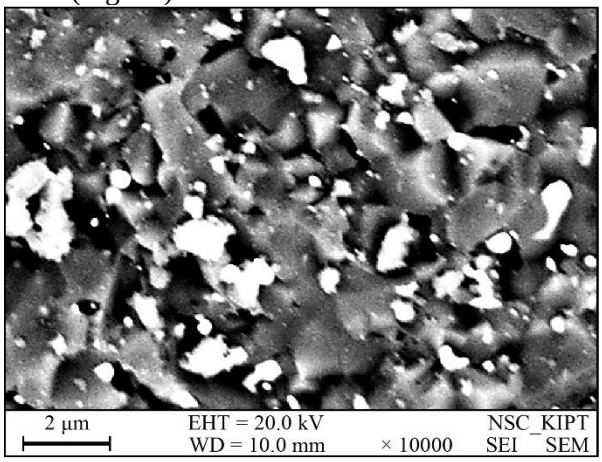

Figure 13. Microstructure of Al_2O_3–15 wt.% SiC composites

In Fig. 14 shows the dependence of the change in relative density on temperature at different electrosintering temperatures.

The advantage of using nanodisperse powders in liquid-phase sintering is to lower the sintering temperature while maintaining the necessary properties. An increase in the dispersion of the powder increases the defectivity of its crystal lattice and the reserve of

excess energy.

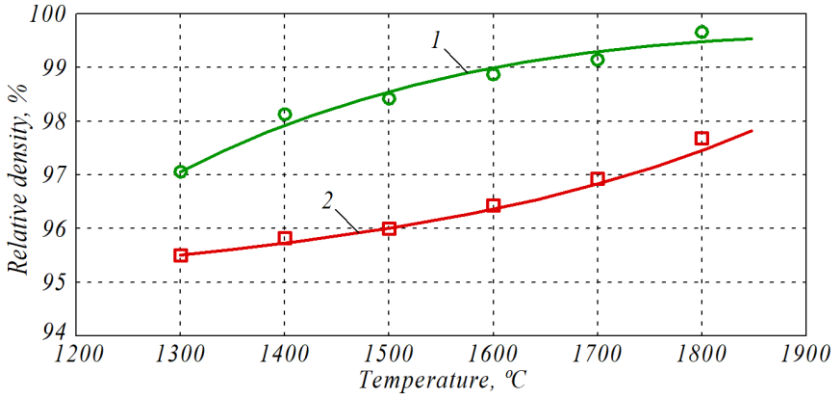

Figure 14. Relative densites CMCs Al_2O_3–15 wt.% SiC under different temperature during electrosintering: *1* – SiC (nano); *2* – SiC (micro)

An increase in the surface layer with distorted lattices promotes the flow of surface diffusion and mass transfer. This approach refers to physical methods of sintering activation.

Grain growth can be controlled by reducing the sintering temperature and holding time, but this causes poor sintering of the particles due to incomplete grain boundary diffusion. As the content of SiC particles in the initial mixture increases, the average grain size decreases. The presence of SiC nanoadditive particles prevents the growth of grains, without requiring a decrease in the sintering temperature and holding time.

4. Conclusions

Obtaining composite materials with high mechanical properties during the consolidation of powder materials is associated with solving a number of difficult tasks. On the one hand, an increase in the sintering temperature promotes a more active course of grain boundary diffusion and their sintering, on the other hand, it activates the formation of by-products, which negatively affects the density and hardness of the material.

When choosing the optimal compaction parameters of composite materials from nanosized powders, special attention should also be paid to their increased activity. But on the other hand, this feature of nanopowders can have a positive effect during liquid-phase sintering, lowering the temperature of eutectic mixture formation.

The study of the mechanical properties of the obtained composites showed that the Al_2O_3–SiC composite reaches the maximum values of microhardness (HV = 25.0 GPa) and crack resistance (K_{IC} = 6.5 MPa·m$^{1/2}$) with a composition of 85 wt.% micro-Al_2O_3–15 wt.% nano-SiC, sintering temperature T_s = 1600 °C, exposure time t = 2 min.

Funding: The researches were co-financed by Ministry of Education and Science of Ukraine project No. 0121U109441.

References

1. M. Cao, Y. Liu, S. Sun, H. Zhou, X. Meng, C. Wang, Effect of Al2O3 micro-powder size on mechanical properties and mi-crostructure of Al2O3-SiC composite ceramic. Ceramics International 41 (2015) 5533–5539. DOI: 10.1016/j.ceramint.2014.12.048.

2. S.L. Cai, X.M. Lu, X.L. Wang, X.C. Hu, Microstructure and mechanical properties of Al2O3/SiC nanocomposite ceramics. Journal of Alloys and Compounds 662 (2016) 85–91. DOI: 10.1016/j.jallcom.2015.12.209.

3. W. Li, W. Li, Q. Li, Y. Liu, Z. Zhang, H. Li, Effect of SiC nanopowder on properties and microstructure of Al2O3-SiC composite ceramic. Ceramics International 44 (2018) 9652–9657. DOI: 10.1016/j.ceramint.2018.02.197.

4. A. Sharma, A. Thakur, R.K. Dutta, Effect of SiC reinforcement on Al2O3 matrix by powder metallurgy technique. Materials Today: Proceedings 5 (2018) 11313–11319. DOI: 10.1016/j.matpr.2018.03.157.

5. S.K. Padhi, S.C. Panigrahi, S.K. Sahoo, Mechanical and tribological behaviour of Al2O3-SiC composite: A review. Tribology - Materials, Surfaces & Interfaces 14 (2020) 97–105. DOI: 10.1080/17515831.2020.1778767.

6. G. Karadimas, K. Salonitis, Ceramic matrix composites for aero engine applications—a review. Applied Sciences 13 (2023) 3017. DOI: 10.3390/app13053017.

7. S. Marimuthu, J. Dunleavey, Y. Liu, M. Antar, B. Smith, Laser cutting of aluminium-alumina metal matrix composite. Optics & Laser Technology 117 (2019) 251–259. DOI: 10.1016/j.optlastec.2019.04.029.

8. C. Bach, F. Wehner, J. Sieder-Katzmann, Investigations on an all-oxide ceramic composites based on Al2O3 fibres and alumina–zirconia matrix for application in liquid rocket engines. Aerospace 9 (2022) 684. DOI: 10.3390/aerospace9110684.

9. P. Putyra, M. Podsiadlo, B. Smuk, Alumina-Ti(C,N) ceramics with TiB2 additives. Archives of Materials Science and Engineering 47/1 (2011) 27–32.

10. L.A. Dobrzanski, M. Kremzer, A. Nagel, B. Huchler, Fabrication of ceramic preforms based on Al2O3 CL 2500 powder. Journal of Achievements in Materials and Manufacturing Engineering 18 (2006) 71–74.

11. E. Gevorkyan, A. Mamalis, R. Vovk, Z. Semiatkowski, D. Morozow, V. Nerubatskyi, O. Morozova, Special features of manufacturing cutting inserts from nanocomposite material Al2O3-SiC. Journal of Instrumentation 16, 10 (2021) P10015. DOI: 10.1088/1748-0221/16/10/P10015.

12. E.S. Gevorkyan, V.P. Nerubatskyi, R.V. Vovk, O.M. Morozova, V.O. Chyshkala, Yu.G. Gutsalenko, Revealing thermomechanical properties of Al2O3–C–SiC composites at sintering. Functional Materials 29, 2 (2022) 193–201. DOI: 10.15407/fm29.02.193.

13. Z. Krzysiak, E. Gevorkyan, V. Nerubatskyi, M. Rucki, V. Chyshkala, J. Caban, T. Mazur, Peculiarities of the phase formation during electroconsolidation of Al2O3–SiO2–ZrO2 powders mixtures. Materials 15, 17 (2022) 6073. DOI: 10.3390/ma15176073.

14. E.S. Gevorkyan, V.P. Nerubatskyi, R.V. Vovk, V.O. Chyshkala, M.V. Kislitsa, Structure formation in silicon carbide – alumina composites during electroconsolidation. Journal of Superhard Materials 44, 5 (2022) 339–349. DOI: 10.3103/S1063457622050033.

15. D. Sofronov, A. Krasnopyorova, N. Efimova, A. Oreshina, E. Bryleva, G. Yuhno, S. Lavrynenko, M. Rucki, Extraction of radionuclides of cerium, europium, cobalt and strontium with Mn3O4, MnO2, and MNOOH sorbents. Process Safety and Environmental Protection 125 (2019) 157–163. DOI: 10.1016/j.psep.2019.03.013.

16. E. Gevorkyan, L. Cepova, M. Rucki, V. Nerubatskyi, D. Morozow, W. Zurowski, V. Barsamyan, K. Kouril, Activated sintering of Cr2O3-based composites by hot pressing. Materials 15, 17 (2022) 5960. DOI: 10.3390/ma15175960.

17. V.P. Nerubatskyi, R.V. Vovk, M. Gzik-Szumiata, E.S. Gevorkyan, Investigation of the effect of

silicon carbide nanoadditives on the structure and properties of microfine corundum during electroconsolidation. Fizika Nizkikh Temperatur 49, 4 (2023) 540–546.

18. J. Merisalu, T. Jogiaas, T.D. Viskus, A. Kasikov, P. Ritslaid, T. Kaambre, A. Tarre, J. Kozlova, H. Mandar, A. Tamm, Structure and electrical properties of zirconium-aluminum-oxide films engineered by atomic layer deposition. Coatings 12 (2022) 431. DOI: 10.3390/coatings12040431.

19. E. Gevorkyan, V. Nerubatskyi, Yu. Gutsalenko, O. Melnik, L. Voloshyna, Examination of patterns in obtaining porous structures from submicron aluminum oxide powder and its mixtures. Eastern-European Journal of Enterprise Technologies 6, 6(108) (2020) 41–49. DOI: 10.15587/1729-4061.2020.216733.

20. E. Gevorkyan, V. Nerubatskyi, V. Chyshkala, O. Morozova, Revealing specific features of structure formation in composites based on nanopowders of synthesized zirconium dioxide. Eastern-European Journal of Enterprise Technologies 5, 12(113) (2021) 6–19. DOI: 10.15587/1729-4061.2021.242503.

21. E.S. Gevorkyan, M. Rucki, A.A. Kagramanyan, V.P. Nerubatskiy, Composite material for instrumental applications based on micro powder Al2O3 with additives nano-powder SiC. International Journal of Refractory Metals and Hard Materials 82 (2019) 336–339. DOI: 10.1016/j.ijrmhm.2019.05.010.

22. M.I. Abd El Aal, H.H. El-Fahhar, A.Y. Mohamed, E.A. Gadallah, The mechanical properties of aluminum metal matrix composites processed by high-pressure torsion and powder metallurgy. Materials 15 (2022) 8827. DOI: 10.3390/ma15248827.

23. K. Raja, V. Sridhar, Mechanical performance of nano-copper reinforced with SiC, AL2O3 using powder metallurgy process. Journal of Emerging Technologies and Innovative Research 6, 5 (2019) 569–574. https://www.jetir.org/papers/JETIRCU06111.pdf.

24. O. Fomin, A. Lovska, V. Pistek, P. Kucera, Research of stability of containers in the combined trains during transportation by railroad ferry. MM Science Journal (2020) 3728–3733. DOI: 10.17973/MMSJ.2020_03_2019043.

25. O. Fomin, A. Lovska, V. Masliyev, A. Tsymbaliuk, O. Burlutski, Determining strength indicators for the bearing structure of a covered wagon's body made from round pipes when transported by a railroad ferry. Eastern-European Journal of Enterprise Technologies 1, 7(97) (2019) 33–40. DOI: 10.15587/1729-4061.2019.154282.

26. E. Gevorkyan, M. Rucki, Z. Krzysiak, V. Chishkala, W. Zurowski, W. Kucharczyk, V. Barsamyan, V. Nerubatskyi, T. Mazur, D. Morozow, Z. Siemiatkowski, J. Caban, Analysis of the electroconsolidation process of fine-dispersed structures out of hot pressed Al2O3–WC nanopowders. Materials 14, 21 (2021) 6503. DOI: 10.3390/ma14216503.

27. E. Gevorkyan, V. Nerubatskyi, V. Chyshkala, Y. Gutsalenko, O. Morozova, Determining the influence of ultra-dispersed aluminum nitride impurities on the structure and physical-mechanical properties of tool ceramics. Eastern-European Journal of Enterprise Technologies 6, 12(114) (2021) 40–52. DOI: 10.15587/1729-4061.2021.245938.

28. V.A. Lapitskaya, T.A. Kuznetsova, A.V. Khabarava, S.A. Chizhik, S.M. Aizikovich, E.V. Sadyrin, B.I. Mitrin, W. Sun, The use of AFM in assessing the crack resistance of silicon wafers of various orientations. Engineering Fracture Mechanics (2021) 107926. DOI: 10.1016/j.engfracmech.2021.107926.

29. D.V. Prosvirnin, M.E. Prutskov, M.D. Larionov, A.G. Kolmakov, Evaluation of the method of measuring crack resistance by the introduction of the vickers indentor for aluminum oxynitride ceramics. Journal of Physics: Conference Series 1431 (2020) 012047. DOI: 10.1088/1742-6596/1431/1/012047.

30. O.P. Umans′kyi, A.H. Dovhal′, A.D. Panasyuk, O.D. Kostenko, Vplyv skladu i struktury kompozytsiynoyi keramiky na osnovi karbidu kremniyu na mekhanizmy znoshuvannya. Poroshkova metalurhiya 07/08 (2012) 92–102 (in Ukrainian).